Monthly Notices
of the
ROYAL ASTRONOMICAL SOCIETY

MNRAS **497,** 3537–3541 (2020)
Advance Access publication 2020 July 27

doi:10.1093/mnras/staa2189

Magnetic fields from cosmological bulk flows

J. A. R. Cembranos,★ A. L. Maroto★ and H. Villarrubia-Rojo ★

Departamento de Física Teórica and Instituto de Física de Partículas y del Cosmos IPARCOS, Universidad Complutense de Madrid, E-28040 Madrid, Spain

Accepted 2020 July 20. Received 2020 July 20; in original form 2020 March 18

ABSTRACT

We explore the possibility that matter bulk flows could generate the required vorticity in the electron–proton–photon plasma to source cosmic magnetic fields through the Harrison mechanism. We analyse the coupled set of perturbed Maxwell and Boltzmann equations for a plasma in which the matter and radiation components exhibit relative bulk motions at the background level. These background bulk motions induce a relative velocity between the matter and cosmic microwave background rest frames at the present time, i.e. a bulk flow, with an amplitude β. We find that, to first order in cosmological perturbations, bulk flows with velocities compatible with current Planck limits ($\beta < 8.5 \times 10^{-4}$ at 95 per cent CL) could generate magnetic fields with an amplitude 10^{-21} G on 10 kpc comoving scales at the time of completed galaxy formation that could be sufficient to seed a galactic dynamo mechanism.

Key words: galaxies: magnetic fields – dark energy – dark matter – cosmology: theory.

1 INTRODUCTION

The origin of the magnetic fields with strengths in the range of the μG found in galaxies and permeating the intergalactic medium in clusters is a long-standing question in astrophysics and cosmology (Widrow 2002). Even more puzzling is the presence of magnetic fields in voids with strengths 3×10^{-16} G as those detected in Neronov & Vovk (2010). The evolution of primordially generated magnetic fields from the early Universe to the onset of structure formation seems to be well understood (Banerjee & Jedamzik 2004; Durrer & Neronov 2013; Subramanian 2016), and there are compelling astrophysical mechanisms, i.e. dynamos, that can amplify a pre-existing magnetic field several orders of magnitude (Davis, Lilley & Tornkvist 1999; Widrow 2002). However, a definite mechanism that can *produce* the primordial seed fields is still lacking.

There are different proposed solutions, which can be classified as cosmological or astrophysical, addressing the origin of the primordial fields. In the cosmological mechanisms, magnetic fields are generated in the early Universe, typically during inflation (Turner & Widrow 1988; Maroto 2001) or in the electroweak (Vachaspati 1991) or quantum chromodynamics (QCD) (Quashnock, Loeb & Spergel 1989) phase transitions. On the other hand, in astrophysical mechanisms, magnetic fields are generated by motions in the plasma during galaxy formation. In general, the amplitude of the seeds generated by these mechanisms is too small to explain the observed fields even with dynamo amplification. Depending on the dynamo amplification rate, a seed field with a strength in the range 10^{-23}–10^{-16} G at galaxy formation and coherent on comoving scales of 10 kpc is required to reach the amplitude of the detected galactic fields Davis et al. (1999).

Among the astrophysical proposals, a particularly appealing one is the so-called Harrison mechanism. In his pioneering work (Harrison 1970), Harrison realized that vorticity in the photon–baryon plasma would lead to the production of electromagnetic fields. The main obstacle (Rees 1987) for the Harrison mechanism to work is to achieve vortical motions in the fluid. Within ΛCDM, to first order in perturbation theory, vorticity and vector modes decay so, even if they are initially large, only small magnetic fields can be generated (Ichiki, Takahashi & Sugiyama 2012). Different routes have been explored to overcome this difficulty. It is possible to source vector modes, e.g. via topological defects, but it was shown in Hollenstein et al. (2008) that if vorticity is transferred only by gravitational interactions, it does not lead to production of magnetic fields. On the other hand, vorticity and magnetic fields are indeed generated to second order in perturbation theory in standard ΛCDM (Takahashi et al. 2005; Fenu, Pitrou & Maartens 2011; Saga et al. 2015), but are consequently very small.

Recently, it has been shown that vorticity in the photon–baryon plasma can also be produced if bulks flows of matter with respect to radiation are present (Cembranos, Maroto & Villarrubia-Rojo 2019). In such a case, first-order scalar metric perturbations induce non-decaying vortical motions in the different plasma components.

The existence of large-scale bulk flows in excess of ΛCDM predictions has been a matter of debate in recent years. While some papers claim to find evidence of unusually large flows (Kashlinsky et al. 2009; Atrio-Barandela et al. 2015), most of the works find results consistent with ΛCDM (Planck Collaboration XIII 2014; Scrimgeour et al. 2016). In particular, the largest scale limits to date on the amplitude of the bulk flow has been set by Planck collaboration XIII (2014) from measurements of the kinetic Sunyaev–Zeldovich effect in clusters and is given by $\beta < 8.5 \times 10^{-4}$ at 95 per cent CL on 2 Gpc scales.

In this work, we find that even a small background bulk velocity, compatible with the Planck limit, is able to generate vorticity to source magnetic fields above the dynamo threshold through the Harrison mechanism.

★ E-mail: cembra@ucm.es (JARC); maroto@ucm.es (ALM); hectorvi@ucm.es (HV-R)

2 PLASMA SYSTEM

Let us assume a homogeneous plasma system composed of photons, protons, and electrons with background bulk velocities $\boldsymbol{\beta}_\gamma$, $\boldsymbol{\beta}_\mathrm{p}$, and $\boldsymbol{\beta}_\mathrm{e}$, respectively. As shown in Cembranos et al. (2019), to first order in β it is always possible to find a centre of mass frame in which the metric takes the Robertson–Walker (RW) form. Thus, including scalar perturbations in the Newtonian gauge the metric reads

$$\mathrm{d}s^2 = a^2(\tau)\{-(1+2\psi)\,\mathrm{d}\tau^2 + (1-2\phi)\,\mathrm{d}\boldsymbol{x}^2\}, \tag{1}$$

and the perturbed fluid velocities can be written as $\boldsymbol{v}_s = \boldsymbol{\beta}_s + \delta\boldsymbol{v}_s$ with $s = \gamma$, e, p. In the following, we will work to first order in bulk velocities and first order in scalar metric perturbations, ignoring the contribution of vector and tensor modes, which, as shown in (Cembranos et al. 2019), would appear as $\mathcal{O}(\beta^2)$ corrections.

The behaviour of the electron–proton–photon plasma is described by a set of coupled Boltzmann equations, which, in a locally inertial frame ($\mathrm{d}t \equiv a(1+\psi)\mathrm{d}\tau$), reads (Cembranos et al. 2019)

$$\frac{Df_\gamma}{\mathrm{d}t} = \mathcal{C}_{\gamma\mathrm{e}}[f_\gamma] + \mathcal{C}_{\gamma\mathrm{p}}[f_\gamma], \tag{2a}$$

$$\frac{Df_\mathrm{e}}{\mathrm{d}t} = \mathcal{C}_{\mathrm{e}\gamma}[f_\mathrm{e}] + \mathcal{C}_{\mathrm{ep}}[f_\mathrm{e}], \tag{2b}$$

$$\frac{Df_\mathrm{p}}{\mathrm{d}t} = \mathcal{C}_{\mathrm{p}\gamma}[f_\mathrm{p}] + \mathcal{C}_{\mathrm{pe}}[f_\mathrm{p}], \tag{2c}$$

where the collision terms take into account both Thomson scattering and the Coulomb interaction between electrons and protons. The evolution of the momentum of the fluids can be followed performing the appropiate integrals over the phase-space distributions. Expressing the results in conformal time τ, integrating over the comoving momentum q^i, and defining

$$\frac{DQ_s^i}{\mathrm{d}\tau} \equiv 2a^{-4}\int \frac{\mathrm{d}^3q}{(2\pi)^3} q^i \frac{Df_s}{\mathrm{d}\tau}, \qquad s = \gamma, \mathrm{e}, \mathrm{p}. \tag{3}$$

we have

$$\frac{DQ_\gamma^i}{\mathrm{d}\tau} = C_{\gamma\mathrm{e}}^i + C_{\gamma\mathrm{p}}^i, \tag{4a}$$

$$\frac{DQ_\mathrm{e}^i}{\mathrm{d}\tau} = C_{\mathrm{e}\gamma}^i + C_{\mathrm{ep}}^i, \tag{4b}$$

$$\frac{DQ_\mathrm{p}^i}{\mathrm{d}\tau} = C_{\mathrm{p}\gamma}^i + C_{\mathrm{pe}}^i. \tag{4c}$$

Additionally, from momentum conservation in Coulomb and Thomson scattering we have $C_{s_1s_2}^i = -C_{s_2s_1}^i$. The electron coupling due to Thomson scattering is (Cembranos et al. 2019)

$$C_{\gamma\mathrm{e}}^i = \frac{4}{3}\rho_\gamma a n_\mathrm{e}\sigma_T\left(\Delta\beta_{\gamma\mathrm{e}}^i + \Delta v_{\gamma\mathrm{e}}^i + \beta_\gamma^i\delta_{n_\mathrm{e}} - \beta_\mathrm{e}^i\delta_\gamma - \frac{3}{4}\beta_{\mathrm{e}\,j}\pi_\gamma^{ij} + \Delta\beta_{\gamma\mathrm{e}}^i\psi\right), \tag{5}$$

where $\delta_{n_\mathrm{e}} = \delta n_\mathrm{e}/n_\mathrm{e}$ is the perturbation of the number of free electrons and π_γ^{ij} is the photon shear tensor. The corresponding Thomson coupling between protons and photons can be obtained with the substitution $\mathrm{e} \to \mathrm{p}$ and $\sigma_\mathrm{T} \to (m_\mathrm{e}/m_\mathrm{p})^2\sigma_\mathrm{T}$. The coupling due to Coulomb scattering takes a similar form (Fenu et al. 2011)

$$C_\mathrm{ep}^i = -e^2 a n_\mathrm{p} n_\mathrm{e}\eta_\mathrm{C}\left(\Delta\beta_\mathrm{ep}^i + \Delta v_\mathrm{ep}^i + \Delta\beta_\mathrm{ep}^i\delta_{n_\mathrm{e}} - \beta_\mathrm{e}^i\Delta n_\mathrm{ep} + \Delta\beta_\mathrm{ep}^i\psi\right), \tag{6}$$

where η_C is the electrical resistivity and we have defined, for two species a and b, the following quantities:

$$\Delta n_{ab} \equiv \delta_{n_a} - \delta_{n_b}, \quad \Delta\beta_{ab}^i \equiv \beta_a^i - \beta_b^i, \quad \Delta v_{ab}^i \equiv \delta v_a^i - \delta v_b^i. \tag{7}$$

The left-hand side of the Boltzmann equation (3) can be splitted into the usual geodesic evolution plus a term taking into account the presence of macroscopic electromagnetic fields. We define the electric and magnetic components of the electromagnetic strength $F_{\mu\nu}$ in the perturbed RW metric as $\mathcal{E}_i = (1+\phi)F_{i0}$ and $\mathcal{B}_i = \frac{1}{2}\varepsilon^{ijk}F_{jk}$. These fields affect the motion of charged particles through the Lorentz force, which takes the standard form

$$\left(\frac{\mathrm{d}q_i}{\mathrm{d}\tau}\right)_\mathrm{EM} = e\left(\mathcal{E}_i + \varepsilon_{ijk}\frac{q^j}{\epsilon}\mathcal{B}^k\right). \tag{8}$$

where $\epsilon \equiv \sqrt{m^2a^2 + q^2}$ is the comoving energy. Notice that, in the absence of bulk flows, scalar perturbations cannot generate magnetic fields to first order in perturbation theory. Therefore, in our scenario, $\mathcal{B}^i$ can only arise as a cross-product of β^i with perturbations. The electric field, on the other hand, can be splitted into a homogeneous piece of $\mathcal{O}(\beta)$ and a perturbation, $\mathcal{E}^i = \mathcal{E}_{(\beta)}^i + \delta\mathcal{E}^i$. Adding the electromagnetic force to equation (4b), the evolution of the velocity of the electrons is

$$m_\mathrm{e}n_\mathrm{e}\Big\{(\partial_\tau + \alpha + \mathcal{H})\left(\beta_\mathrm{e}^i + \delta v_\mathrm{e}^i\right) + \left(\beta_\mathrm{e}^i\delta_k^j + \beta_\mathrm{e}^j\delta_k^i\right)\partial_j\delta v_\mathrm{e}^k + \partial^i\psi - 4\beta_\mathrm{e}^i\dot{\phi} + \frac{e}{m_\mathrm{e}a}(1+\delta_{n_\mathrm{e}})\mathcal{E}^i\Big\} = C_{\mathrm{e}\gamma}^i + C_\mathrm{ep}^i. \tag{9}$$

The first line contains, in addition to the usual Hubble dilution term, a coefficient $\alpha = \partial_\tau(a^3n_\mathrm{e})/(a^3n_\mathrm{e})$ representing a possible variation in the comoving number of free electrons at the background level, e.g. due to recombination, and the effective shear stress induced by the bulk motion of the fluid $\pi_{ij} \sim \beta_i\delta v_j$. The second line contains the effect of metric perturbations, both the standard one and the correction induced by the presence of cosmological bulk flows (Cembranos et al. 2019). The metric contribution is irrelevant for the Harrison mechanism, but it will be important to study the evolution of the photon–baryon plasma vorticity. Finally, the last term takes into account the electromagnetic effects. A similar result can be found for protons after changing the relevant subscripts and the electric charge $e \to -e$. Subtracting the equations for electrons and protons, we obtain an expression for the velocity difference:

$$(\partial_\tau + \alpha + \mathcal{H})\left(\Delta\beta_\mathrm{ep}^i + \Delta v_\mathrm{ep}^i\right) + \left(\beta_\mathrm{e}^i\theta_\mathrm{e} + \beta_\mathrm{e}^j\partial_j\delta v_\mathrm{e}^i - (\mathrm{e}\leftrightarrow\mathrm{p})\right) - 4\Delta\beta_\mathrm{ep}^i\dot{\phi} + \frac{e}{m_\mathrm{e}a}\left(\mathcal{E}_{(\beta)}^i + \delta\mathcal{E}^i + \delta_{n_\mathrm{e}}\mathcal{E}_{(\beta)}^i\right) = \frac{1}{m_\mathrm{e}n_\mathrm{e}}\left(C_{\mathrm{e}\gamma}^i + C_\mathrm{ep}^i\right), \tag{10}$$

where we have used the fact that $m_\mathrm{p} \gg m_\mathrm{e}$. Next, we show how this expression, combined with the Maxwell equations, gives rise to magnetic fields.

3 TIME-SCALES

Following Fenu et al. (2011), we define the time-scales relevant for the system (10), assuming a matter-dominated universe.

(i) Electrical resistivity.

$$\eta \equiv \frac{\eta_\mathrm{C}}{a} \simeq \frac{10\pi e^2\sqrt{m_\mathrm{e}}}{aT^{3/2}} \simeq 10^{-9}\ \mathrm{s}\left(\frac{1+z}{10^3}\right)^{-1/2}. \tag{11}$$

(ii) Coulomb time-scale.

$$\tau_\mathrm{C} \equiv \frac{m_\mathrm{e}}{ae^2n_\mathrm{e}\eta_\mathrm{C}} \simeq \frac{2\times10^4\ \mathrm{s}}{x_\mathrm{e}}\left(\frac{1+z}{10^3}\right)^{-1/2}. \tag{12}$$

(iii) Thomson time-scale.

$$\tau_\mathrm{T} \equiv \frac{m_\mathrm{e}}{a\sigma_\mathrm{T}\rho_\gamma} \simeq 5\times10^{11}\ \mathrm{s}\left(\frac{1+z}{10^3}\right)^{-3}. \tag{13}$$

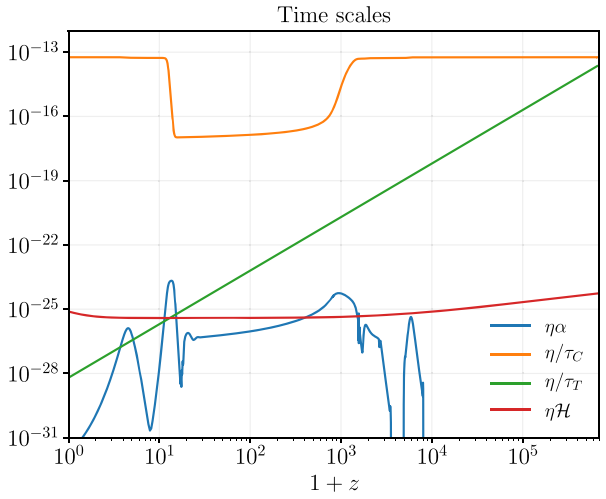

Figure 1. Ratios of the relevant scales of the problem, with respect to the dominant one: the electrical resistivity η. During the period of interest, the next scale in the hierarchy is the Coulomb time-scale. Early enough in time, Thomson scattering becomes more efficient than Coulomb scattering.

There are other time-scales in the problem such as the cosmological ones, $\mathcal{H}^{-1}$ and $k^{-1} \simeq 10^{14}\,\mathrm{s}\,(\mathrm{Mpc}^{-1}\,k^{-1})$, and the time-scale of recombination $\alpha = \dot{x}_\mathrm{e}/x_\mathrm{e}$. The ratio of these scales with respect to η is represented in Fig. 1.

There is a very strong hierarchy of scales, with $\eta \ll \tau_\mathrm{C} \ll \tau_\mathrm{T}, \mathcal{H}^{-1}, \alpha^{-1}$. In the next section, we will use this fact to find an approximate solution of the system.

4 PRODUCTION MECHANISM

The main physical mechanisms at work can be nicely illustrated analysing the behaviour of the bulk velocities. The relevance of the previous time-scales will be made explicit if we write the equations in terms of $e^i_{(\beta)}$, where $\mathcal{E}^i_{(\beta)} = e\,a^{5/2} n_\mathrm{e} \tau_\mathrm{C}\, e^i_{(\beta)}$. At the background level, the leading $\mathcal{O}(\beta)$ piece of equation (10), plus the relevant Maxwell equation, yields

$$\Delta\dot{\beta}^i_\mathrm{ep} + \left(\frac{1}{\tau_\mathrm{c}} + \alpha + \mathcal{H}\right)\Delta\beta^i_\mathrm{ep} + \frac{1}{a^{1/2}\eta}\, e^i_{(\beta)} = \mathcal{T}^i_\beta, \tag{14a}$$

$$\dot{e}^i_{(\beta)} - \frac{a^{1/2}}{\tau_\mathrm{c}}\Delta\beta^i_\mathrm{ep} = 0, \tag{14b}$$

where the Thomson dragging term is $\mathcal{T}^i_\beta \equiv \frac{4}{3\tau_\mathrm{T}}\Delta\beta^i_{\gamma\mathrm{e}}$. The result is a very simple dynamical system where, as discussed in the previous section, the strong hierarchy of scales present in the problem allows us to simplify the analysis keeping only the leading $\mathcal{O}(\eta)$ behaviour. The homogeneous part of this system (without the source) corresponds to the usual electron–proton plasma (without photons). If the system is placed out of the equilibrium $\Delta\beta^i_\mathrm{ep} = e^i_{(\beta)} = 0$ configuration, an electric field is created in response, acting as a restoring force. The homogeneous solutions oscillate with characteristic frequency $\omega \simeq 1/\sqrt{\eta\,\tau_\mathrm{C}}$ and are damped with a damping coefficient $\Gamma \simeq 1/2\tau_\mathrm{C}$. The presence of photons modifies this picture. Due to the large mass difference, $m_\mathrm{p} \gg m_\mathrm{e}$, the Thomson coupling of photons to electrons is much more effective than to protons, producing a differential dragging and introducing the source $\mathcal{T}^i_\beta$. The particular solution of the system (14) can be found to be

$$\Delta\beta^i_\mathrm{ep} = \eta\,\tau_\mathrm{C}\,\mathcal{T}^i_\beta + \mathcal{O}(\eta^2), \tag{15a}$$

$$e^i_{(\beta)} = a^{1/2}\,\eta\,\mathcal{T}^i_\beta + \mathcal{O}(\eta^2). \tag{15b}$$

This is the essence of the Harrison mechanism: the Thomson dragging of the photons produces an electric field proportional to the photon–baryon velocity difference. Notice that a homogeneous electric field is generated, pointing in the bulk flow direction and with a small amplitude $\mathcal{E}_{(\beta)} \lesssim 10^{-30}\ \mathrm{G}(1+z)^2$, according to the current Planck limits for β. The same kind of analysis can be carried out to prove that $\Delta n_\mathrm{ep}, \Delta v^i_\mathrm{ep} = \mathcal{O}(\eta\,\tau_\mathrm{C})$ and from (10) we get the leading-order result

$$\delta\mathcal{E}^i = \frac{a}{e n_\mathrm{e}} C^i_{\mathrm{e}\gamma} - \delta_{n_\mathrm{e}}\mathcal{E}^i_{(\beta)} + \mathcal{O}(\eta)\,. \tag{16}$$

In Fourier space, we decompose the velocity and the electromagnetic fields into vortical and longitudinal components as

$$\delta\boldsymbol{v}_s = \chi_s(\hat{\beta} - (\hat{\beta}\cdot\hat{k})\,\hat{k}) - \frac{\mathrm{i}}{k}\theta_s\,\hat{k}, \tag{17a}$$

$$\boldsymbol{\mathcal{E}} = \mathcal{E}^\perp(\hat{\beta} - (\hat{\beta}\cdot\hat{k})\,\hat{k}) + \mathcal{E}^\parallel\,\hat{k}, \tag{17b}$$

$$\boldsymbol{\mathcal{B}} = \mathrm{i}\,\mathcal{B}(\hat{\beta}\wedge\hat{k}). \tag{17c}$$

From the Maxwell equations, including perturbations, we have

$$\dot{\mathcal{B}} = -k\,\delta\mathcal{E}^\perp + k\phi\,\mathcal{E}^\perp_{(\beta)}. \tag{18}$$

Plugging in the expression obtained for the electric field (equation 16) and written in terms of the physical magnetic field $\boldsymbol{B} \equiv a^{-2}\boldsymbol{\mathcal{B}}$, which can be obtained projecting with the tetrad of a locally inertial observer (Durrer & Neronov 2013), equation (18) reads

$$\frac{\mathrm{d}}{\mathrm{d}\tau}\left(a^2 B\right) = -\frac{4a^2 k\sigma_\mathrm{T}\rho_\gamma}{3e}\left(\Delta\chi_{\gamma\mathrm{e}} + \beta_\mathrm{e}\left(\delta_{n_\mathrm{e}} - \delta_\gamma - \frac{1}{2}\sigma_\gamma\right) + \Delta\beta_{\gamma\mathrm{e}}(\psi - \phi)\right). \tag{19}$$

This is the final equation governing the production of magnetic fields. It generalizes the Harrison mechanism to the case in which there are bulk flows in the plasma. It is also analogous to the one obtained in previous studies of production of magnetic fields in second-order cosmological perturbation theory (Fenu et al. 2011; Saga et al. 2015). Details on the evolution of the cosmological bulk flows β, and the vorticity produced by these flows can be found in Cembranos et al. (2019).

5 EVOLUTION AND RESULTS

The magnetic field power spectrum is defined by

$$\langle B_i(z,\boldsymbol{k})B^*_j(z,\boldsymbol{k}')\rangle = (2\pi)^3\delta(\boldsymbol{k}-\boldsymbol{k}')(\hat{\beta}\wedge\hat{k})_i(\hat{\beta}\wedge\hat{k})_j\,P_B(z,k), \tag{20}$$

as

$$P_B(z,k) = |T_B(z,k)|^2\frac{2\pi^2}{k^3}\mathcal{P}_\mathcal{R}(k), \tag{21}$$

where $\mathcal{P}_\mathcal{R}(k)$ is the usual nearly scale-invariant primordial curvature power spectrum and $T_B(z,k)$ is the magnetic field transfer function computed using (19). In Figs 2 and 3, the comoving magnetic field $(1+z)^{-2}|T_B|\mathcal{P}^{1/2}_\mathcal{R}$ is plotted as a function of redshift and scale, respectively.

There are two points worth emphasizing. On the one hand, the magnetic power spectrum on small and large scales has a power-law behaviour

$$\sqrt{k^3 P_B(z<100,k)} \propto \begin{cases} k^{1.2}\,, & k \gg 0.1\ \mathrm{Mpc}^{-1}, \\ k^{2.8}\,, & k \ll 0.1\ \mathrm{Mpc}^{-1}, \end{cases} \tag{22}$$

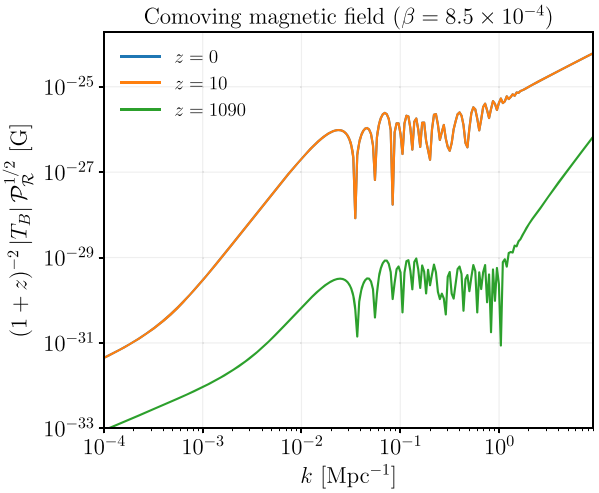

Figure 2. Comoving magnetic field as a function of the scale for different redshifts. Notice that the $z = 0$ and $z = 10$ curves overlap. Even though there is an important production immediately after decoupling, afterwards the comoving magnetic field is constant at all scales and it is not affected by reionization.

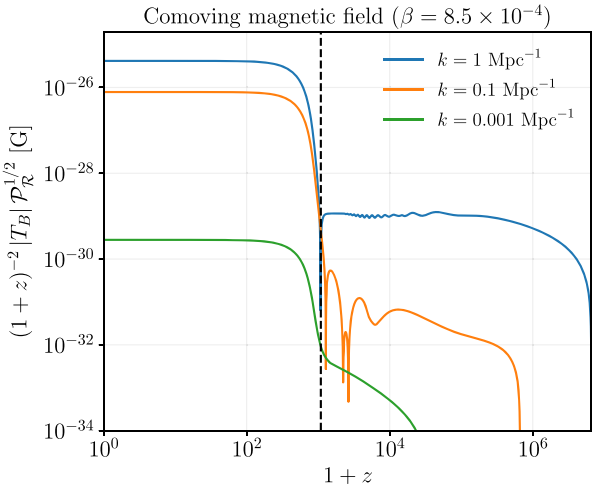

Figure 3. Comoving magnetic field as a function of the redshift for different scales. The magnetic field presents some features inherited from the acoustic oscillations before decoupling. The main production takes place during and immediately after decoupling. Once the photon–baryon plasma is decoupled, the comoving magnetic field is constant.

so that the magnetic field is steeply rising as $k^{1.2}$ on small scales, until the turbulence scale kicks in. On the other hand, the comoving magnetic field is continuously produced, with an important boost at recombination and remaining essentially constant for $z < 100$.

Following Fenu et al. (2011), we also define the magnetic field smoothed over a comoving scale L as

$$B_L^2(z) = \frac{1}{2\pi^2}\int_0^\infty \mathrm{d}k\, k^2 P_B(z,k) \exp\left(-\frac{k^2L^2}{2}\right) . \tag{23}$$

The magnetic field B_L at the time of galaxy formation $z_{\rm gf} = 10$ is depicted in Fig. 4. The numerical computation of the transfer function becomes harder for smaller scales, and some of the usual approximations in cosmic microwave background calculations cannot be trusted for scales $k > 10\,\mathrm{Mpc}^{-1}$ (Blas, Lesgourgues & Tram

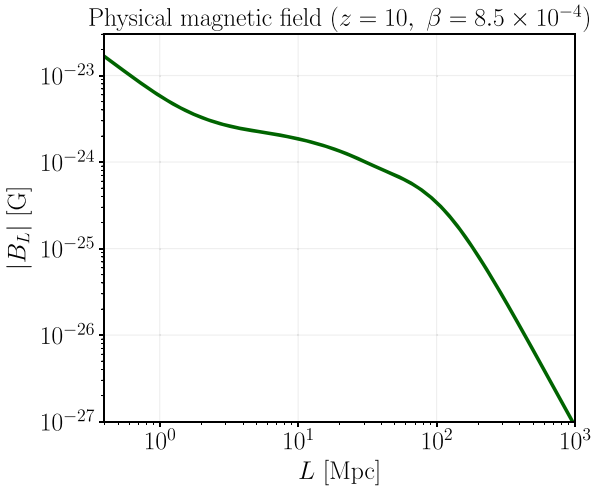

Figure 4. Physical magnetic field smoothed over a given scale L. It is evaluated at a redshift $z = 10$, where the dynamo mechanism should begin to operate Widrow (2002). Since the comoving field is constant at late times, the results can be easily rescaled to any redshift.

2011). Therefore, we only compute the spectrum up to scales $k = 9\,\mathrm{Mpc}^{-1}$. Again, the field B_L can be well approximated as a power law at small and large scales

$$B_L(z<100) \propto \begin{cases} L^{-1.2}\,, & L > 100\ \mathrm{Mpc}\,, \\ L^{-2.8}\,, & L < 2\ \mathrm{Mpc}\,. \end{cases} \tag{24}$$

For intermediate scales, as can be appreciated from Figs 2 and 3, the acoustic oscillations of the plasma imprint a complex pattern in the magnetic field spectrum prior to decoupling. This region of acoustic oscillations roughly corresponds to the scales $2\,\mathrm{Mpc} < L < 100\,\mathrm{Mpc}$ in the smoothed magnetic field in Fig. 4. For small scales, we obtain the following approximate result

$$|B_L(z<100)| \simeq 5.7\times10^{-24}\ \mathrm{G}\left(\frac{L}{\mathrm{Mpc}}\right)^{-1.2} \times \left(\frac{1+z}{11}\right)^2\left(\frac{\beta}{8.5\times10^{-4}}\right), \tag{25}$$

for $L < 1$ Mpc, where β is the relative bulk velocity between photons and baryons. These results show that although the field seems too weak to directly account for the intergalactic magnetic fields or magnetic fields in voids, the mechanism proposed provides a seed field large enough to potentially explain the galactic magnetic fields, after a suitable dynamo amplification.

ACKNOWLEDGEMENTS

This work has been supported by the Ministerio de Economía (MINECO, Spain) project FIS2016-78859-P(AEI/FEDER,UE).

DATA AVAILABILITY

The data used to generate the plots in this article will be shared on reasonable request to the corresponding author.

REFERENCES

Atrio-Barandela F., Kashlinsky A., Ebeling H., Fixsen D. J., Kocevski D., 2015, ApJ, 810, 143

Banerjee R., Jedamzik K., 2004, Phys. Rev. D, 70, 123003
Blas D., Lesgourgues J., Tram T., 2011, J. CAP, 1107, 034
Cembranos J. A. R., Maroto A. L., Villarrubia-Rojo H., 2019, J. Cosmol. Astropart. Phys., 1906, 041
Davis A.-C., Lilley M., Tornkvist O., 1999, Phys. Rev. D, 60, 021301
Durrer R., Neronov A., 2013, A&A Rev., 21, 62
Fenu E., Pitrou C., Maartens R., 2011, MNRAS, 414, 2354
Harrison E., 1970, MNRAS, 147, 279
Hollenstein L., Caprini C., Crittenden R., Maartens R., 2008, Phys. Rev. D, 77, 063517
Ichiki K., Takahashi K., Sugiyama N., 2012, Phys. Rev. D, 85, 043009
Kashlinsky A., Atrio-Barandela F., Kocevski D., Ebeling H., 2009, ApJ, 686, L49
Maroto A. L., 2001, Phys. Rev. D, 64, 083006
Neronov A., Vovk I., 2010, Science, 328, 73
Planck Collaboration XIII, 2014, A&A, 561, A97
Quashnock J. M., Loeb A., Spergel D. N., 1989, ApJ, 344, L49
Rees M. J., 1987, Q. J. R. Astron. Soc., 28, 197
Saga S., Ichiki K., Takahashi K., Sugiyama N., 2015, Phys. Rev. D, 91, 123510
Scrimgeour M. I. et al., 2016, MNRAS, 455, 386
Subramanian K., 2016, Rep. Prog. Phys., 79, 076901
Takahashi K., Ichiki K., Ohno H., Hanayama H., 2005, Phys. Rev. Lett., 95, 121301
Turner M. S., Widrow L. M., 1988, Phys. Rev. D, 37, 2743
Vachaspati T., 1991, Phys. Lett., B265, 258
Widrow L. M., 2002, Rev. Mod. Phys., 74, 775

This paper has been typeset from a TEX/LATEX file prepared by the author.